

The Very Small Array: Observations and Latest Results

Anže Slosar

Astrophysics group, Cavendish Laboratory, Madingley Rd, Cambridge, CB3 0HE, U.K.

Clive Dickinson

Jodrell Bank Observatory, University of Manchester, Macclesfield, Cheshire, SK11 9DL, U.K.

Abstract. The Very Small Array (VSA) is a unique interferometric telescope operating at 33 GHz at Tenerife. It has the ability to measure fluctuations in the CMB over a large range of angular scales by means of three main array configurations: compact, extended and super-extended. These angular scales correspond to the multipole range $\ell = 150 - 2500$. Here we present new results from further observations of the extended array (February 2002 - June 2003). We cover ℓ -values up to $\ell \sim 1600$, thus doubling the ℓ -range of WMAP. The resulting power spectrum in the ℓ -range 800 - 1600 has very low noise coupled with good ℓ -resolution ($\Delta\ell \sim 80$). Furthermore, the use of independently tracking aerials along with the dedicated source subtraction baseline allows unprecedented control of systematics. The latter is essential, since discrete sources are the dominant foreground at these angular scales. These measurements over larger ℓ -ranges are important in confirming the present cosmological paradigm and breaking degeneracies in the extraction of cosmological parameters.

1. Introduction

The measurement of the CMB power spectrum has become a fundamental tool for cosmology. Many experiments have now measured the CMB anisotropies, both acoustic peaks on large angular scales ($\ell < 1000$) (Lee et al. 2001; Netterfield et al. 2002; Halverson et al. 2002; Scott et al. 2003) and the damping tail on smaller angular scales (Pearson et al. 2003; Kuo et al. 2004). The recent Wilkinson Microwave Anisotropy Probe (WMAP) has measured the power spectrum up to $\ell \sim 700$ with unprecedented sensitivity (Bennett et al. 2003a). The new challenge for CMB therefore lies with measuring higher ℓ -values and polarisation. It is crucial that measurements possess enough ℓ -resolution and sensitivity to disentangle peaks, test the current cosmological model and probe new cosmological parameters.

In this paper, we present the latest observations taken with the VSA. This improves on data given in Grainge et al. (2003) with better sensitivity up to $\ell \sim 1600$, complementing WMAP data at lower ℓ -values and adding a unique dataset at higher ℓ values.

2. The Instrument

The VSA is a 14 element interferometer operating in the Ka-band (26 – 36 GHz) and situated at the high and dry site of Izana, Tenerife at an altitude of 2340 m (Watson et al. 2003). The VSA is a collaboration between the Cavendish Astrophysics group (University of Cambridge), Jodrell Bank Observatory (University of Manchester) and the Instituto de Astrofísica de Canarias (IAC, Tenerife). The site was chosen to give minimal atmospheric/weather contamination with transparency of 98 per cent at 30 GHz along with a good infra-structure provided by the IAC. Less than 10 per cent of data are flagged due to weather and the overall observing efficiency is better than 50 per cent.

The nominal specifications for the VSA extended array are given in Table 1. The VSA utilises the best low noise amplifiers at 30 GHz developed by Eddie Blackhurst (JBO) based on a design by Marian Pospieszalski (NRAO), providing 1.5 GHz instantaneous bandwidth and system temperatures of ~ 30 K. The antennas can be placed anywhere on a tip-tilt table which allows us to optimise the array configuration for different angular scales. So far, we have used two configurations: the compact and extended arrays, shown in Figure 1. Future VSA observations will be made in an even larger configuration and bigger mirrors to probe $\ell > 1500$. The compact array was optimised for the larger angular scales ($\ell < 500$) while the current extended array has larger horns and longer baselines to measure higher ℓ -values (500 – 1500) with good temperature sensitivity.

Table 1. Nominal specifications of the VSA extended array.

| | |
|--|-------------------------------------|
| Location | Izana, Tenerife (2340 m) |
| Maximum declination range | $-5^\circ < \text{Dec} < +70^\circ$ |
| No. of antennas (baselines) | 14 (91) |
| Range of baselines | 0.4 m – 2.5 m (4.5 m max.) |
| Frequency range | 26 – 36 GHz |
| System temperature, T_{sys} (K) | ~ 35 K |
| Bandwidth, $\Delta\nu$ | 1.5 GHz |
| Correlator | 91-channel complex correlator |
| Mirror diameter | 322 mm |
| Primary beam | $2^\circ.0$ FWHM at 34 GHz |
| Synthesized beam | ≈ 11 arcmin |
| Range of ℓ | $\sim 300 - 1600$ |
| Flux sensitivity | $\sim 6 \text{ Jy s}^{-1/2}$ |
| Temperature sensitivity | $\sim 15 \text{ mK s}^{-1/2}$ |

The VSA is extremely resistant to systematic effects. This is partly due to properties inherent to interferometry such as the primary beam envelope, the automatic rejection of the “DC” component and a unique modulation of the astronomical signal known as astronomical fringe-rate. The VSA has negligible beam uncertainties and pointing errors. The VSA can reject known signals by application of Fourier filtering. This is applied to data when the Sun and Moon are within 27 and 18 degrees respectively. An example of the Fourier filtering is shown in Figure 2. Unlike other CMB interferometers, this allows real maps

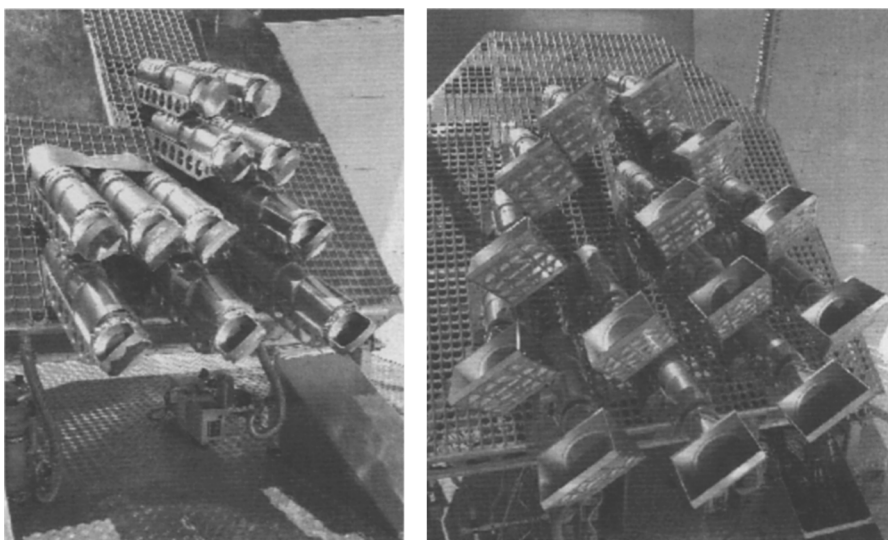


Figure 1. The VSA main array shown in the compact array (left) during the commissioning period (May 2000) with 11 antennas on the tip-tilt table and the extended array (right) with 14 antennas in October 2001. The main table is situated inside a metal enclosure to minimise ground spillover.

to be constructed from the data (rather than maps of the sky difference). This also allows 24 hour observations to be made.

3. Observations

The results presented here are based mainly on observations made during October 2001 – June 2003 in the extended configuration. The observations consist of a total of 33 pointings that make up three 7-field mosaics and four 3-field mosaics. The 7-field mosaics are placed on a regular hexagon with a field on each vertex and the 7th field at the centre of the hexagon. The 3-field mosaics are placed on an equilateral triangle. The distance between adjacent fields is 1.25° in both cases. The fields were carefully chosen to limit the contamination from foreground emissions (discussed in section 5) and to give even distributions in Right Ascension to allow 24-hour observing. To constrain the lowest ℓ part of the spectrum, we have included the compact array dataset (Taylor et al. 2003) in the analysis.

4. Data Reduction and Calibration

The VSA data reduction pipeline has been developed over several years and is now almost all fully automated. To minimise the subjectiveness in the remaining manual part of the data reduction process (manual flagging, selection of the most appropriate calibrator, etc.), the reduction has been done redundantly across the

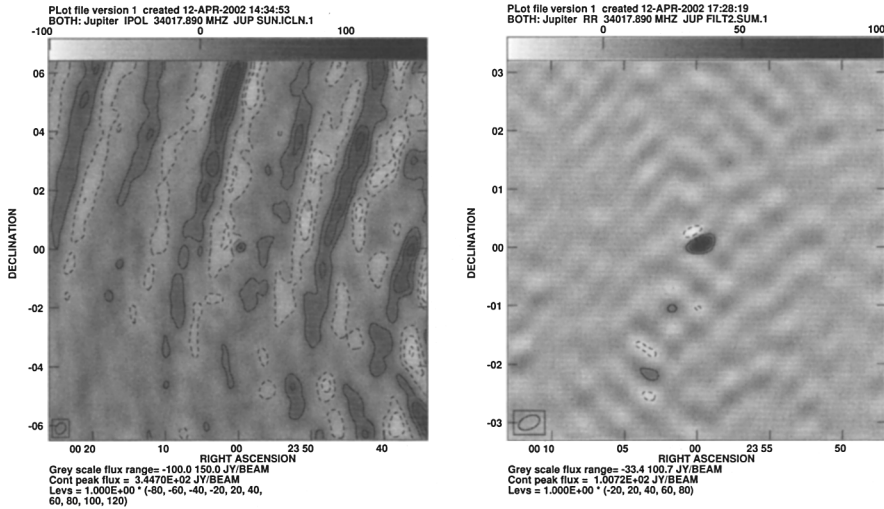


Figure 2. Example of Fourier filtering. *Left*: observation of Jupiter (100 Jy) with a Sun separation of 11° . The diffraction rings from the Sun can be seen clearly. *Right*: The same data with Fourier filtering applied. The stripes are completely removed and Jupiter is recovered accurately. The remaining noise features are consistent with the predicted thermal noise of the instrument.

three collaborating institutions so that each field was reduced independently by at least two groups.

Calibration of VSA data is achieved by observing bright calibrator sources. The VSA is extremely phase stable (Rusholme 2001; Watson et al. 2003) which allows accurate amplitude and phase corrections to be calculated from a single calibrator observation. A further correction is made for the atmospheric attenuation using noise diodes injected into each antenna. This typically corresponds to a correction of a few per cent. Data containing larger corrections are flagged on the assumption that the data will be either noisy or badly affected by weather.

The absolute calibration of VSA data is calculated with respect to Jupiter. In previous papers, we have used $T_J = 152 \pm 5$ K (Mason et al. 1999) which gives an error of ~ 3 per cent accuracy in temperature and 6 per cent in the power spectrum. The recent results from WMAP provide a new and more accurate absolute scale. We therefore use $T_J = 146.6 \pm 2.0$ K (Page et al. 2003) corresponding to an accuracy of 1.4 per cent in temperature or 2.8 per cent accuracy in the power spectrum. We quote 3 per cent as our calibration uncertainty. Compared to earlier VSA data, this is a scaling down of 8 per cent in the power spectrum.

5. Foregrounds

5.1. Discrete Radio Sources

The dominant foreground for the VSA at 33 GHz is discrete radio sources. However, there are no large surveys available at these frequencies. We avoid the brightest sources (above 500 mJy) by careful choice of fields. However, source contamination increases as ℓ^2 in the power spectrum. This means that at higher ℓ -values, the foreground contamination from sources must be accurately subtracted. We do this using a 2-stage dedicated source-subtraction system. The first stage involves surveying the VSA regions using the Ryle Telescope (Cambridge) at 15 GHz. The second stage is to observe the identified sources at the same frequency (33 GHz) *and* at the same time to account for variability in some of the sources. This is achieved by employing two 3.7 m dishes separated by 9 m working as a single baseline interferometer.

The results of the extended array 33 GHz monitoring programme will be given by Cleary et al. (in preparation). In summary, we monitor ~ 100 sources in each 2° field. Many of these are too faint to detect because a large population have steep spectral indices making them very faint at high frequencies. Only sources above 20 mJy are accurately measured and subtracted from the data. This removes the dominant component of sources and leaves a small residual signal from sources below the completeness limit of the monitoring programme. These are subtracted statistically using the Toffolatti model (Toffolatti et al. 1998) scaled using our own measurements of the source counts at 33 GHz: $\Delta T_{\text{sr}\ell}^2 = \ell(\ell + 1)1.22 \times 10^{-3}/2\pi$. This corresponds to a correction of $194 \times (\ell/1000)^2 \mu\text{K}^2$.

5.2. Galactic Foregrounds

For the VSA at 33 GHz, the contamination from Galactic foregrounds is relatively small compared to the CMB signal and the current noise levels in VSA data. Galactic emissions consist of synchrotron, free-free and dust emission. Galactic foregrounds are minimised by careful choice of fields based on the 408 MHz all-sky map (Haslam et al. 1981) which traces synchrotron emission and the FIR 100 μm DIRBE/IRAS map given by Schlegel, Finkbeiner, & Davis (1998) which is a good tracer of dust. This results in most of the VSA fields located at high Galactic latitudes ($|b| > 30^\circ$). Furthermore, the interferometer response means that large scale power from the Galaxy is not measured.

The current synchrotron templates (Haslam et al. 1981) and free-free templates (Dickinson, Davies, & Davis 2003; Finkbeiner 2003) are not well suited to the VSA since they do not have the required resolution (< 10 arcmin). However, based on recent analyses of the COBE-DMR data (Banday et al. 2003) and WMAP data (Bennett et al. 2003b), the largest foregrounds at frequencies of $\sim 20 - 40$ GHz, are those correlated with the FIR. We therefore choose to use the Schlegel, Finkbeiner, & Davis (1998) 100 μm map as a tracer of all the Galactic foregrounds.

We simulate VSA observations based on the 100 μm maps for each of the VSA regions taking into account the VSA u, v coverage and primary beams. The power spectra from these simulations are then calculated with an arbitrary scaling. The scaling coefficient from FIR map units (MJy sr^{-1}) to brightness

temperature (μK) has substantial variations with typical values lying between $5 - 30 \mu\text{K}/(\text{MJy sr}^{-1})$. We therefore apply a nominal correction based on the average scaling coefficient for these regions which is $\approx 10 \mu\text{K}/(\text{MJy sr}^{-1})$. The correction is then given by $\Delta T_{\text{Gal}}^2 = 28 \times (\ell/1000)^{-0.72} \mu\text{K}^2$.

6. Results

Maps for three 7-field mosaics observed by the VSA are shown in Figure 3.

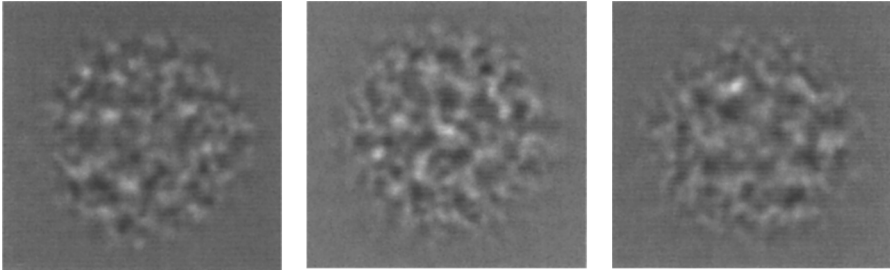


Figure 3. MEM reconstructions of all three 7-field mosaics observed by the VSA (VSA1/VSA2/VSA3). Signal to noise at the centre of each of these maps is around 3.

The CMB power spectrum is estimated from visibilities using the MAD-COW package (Hobson & Masinger 2002). The power spectrum from all VSA data is presented in Figure 4. In the region of overlap, the WMAP and VSA data agree exceptionally well. The VSA data suggest a hint of the 3rd and 4th peaks where the power has already dropped dramatically with ℓ as predicted by the standard cosmological models.

7. Conclusions and Future Plans

The new VSA dataset provides an accurate and independent measurement of the angular power spectrum of fluctuations in the Cosmic Microwave Background in the multipole range $\ell = 150 - 1600$. The measurements sample the adiabatic peaks with a good ℓ resolution and are fully consistent with theoretical predictions for a concordance cosmological model.

These data and power spectrum are more thoroughly investigated in Dickinson et al. (2004) while the cosmological implications of these new data is given by Rubiño-Martin et al. (2003).

The future of the VSA lies in measuring even higher ℓ values while maintaining good $\Delta\ell$ resolution, which is necessary in order to Nyquist-sample the acoustic peaks present in the power spectrum. Another important task is to investigate the excess power seen in the CBI data (Mason et al. 2003). The real imaging capability of the VSA, coupled with the source subtraction system will allow the VSA to independently confirm this excess and investigate its properties. To achieve this, the telescope will be upgraded in three aspects. Firstly, even bigger reflectors that couple efficiently to the angular scales corresponding

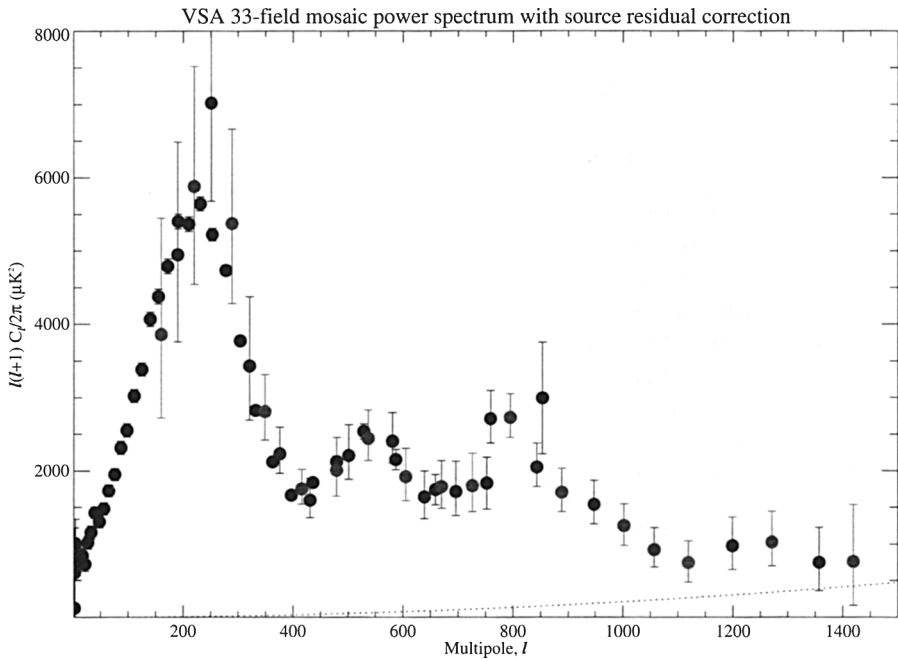


Figure 4. The CMB power spectrum from the VSA is plotted in grey for two sets of bins. The 1st-year WMAP data (black circles) are plotted for comparison. The thin dotted line indicates the level of the residual point source correction.

to $\ell = 1000 - 2500$ will be installed (super-extended array). Secondly, the front-end amplifiers will be replaced, decreasing the system temperature from 35K to 25K. Finally, the system will be broad-banded from 1.5 GHz to 8 GHz. This will bring the VSA back to the cutting edge of experimental efforts in the CMB.

Acknowledgments. We thank all members of the VSA team from all three institutions for the hard work that has gone into the VSA project. We thank PPARC for funding and supporting the VSA project. A particular mention goes to Dr. R. A. Watson (IAC) for his work in not only in analysing the data but also for his weekly efforts keeping the telescope working at full efficiency.

References

- Banday, A. J., Dickinson, C., Davies, R. D., Davis, R. J., & Gorski, K. M. 2003, *MNRAS*, 345, 897
- Bennett, C. L., et al. 2003a, *ApJS*, 148, 1
- Bennett, C. L., et al. 2003b, *ApJS*, 148, 97
- Dickinson, C., Davies, R. D., & Davis, R. J. 2003, *MNRAS*, 341, 369
- Dickinson, C., et al. 2004, *MNRAS*, 353, 732
- Finkbeiner, D. P. 2003, *ApJS*, 146, 407
- Grainge, K. J. B., et al. 2003, *MNRAS*, 341, L23

- Halverson, N. W., et al. 2002, *ApJ*, 568, 38
Haslam, C. G. T., et al. 1981, *A&A*, 100, 209
Hobson, M. P., & Maisinger K. 2002, *MNRAS*, 334, 569
Kuo, C. L., et al. 2004, *ApJ*, 600, 32
Lee, A. T., et al. 2001, *ApJ*, 561, L1
Mason, B. S., Leitch, E. M., Myers, S. T., Cartwright, J. K., & Readhead, A. C. S. 1999, *AJ*, 118, 2908
Mason, B. S., et al. 2003, *ApJ*, 591, 540
Netterfield, C. B., et al. 2002, *ApJ*, 571, 604
Page, L., et al. 2003, *ApJS*, 148, 39
Pearson, T. J., et al. 2003, *ApJ*, 591, 556
Rubino-Martin, J. A., et al. 2003, *MNRAS*, 341, 1084
Rusholme, B. 2001, PhD thesis, University of Cambridge
Schlegel, D. J., Finkbeiner, D. P., & Davis, M. 1998, *ApJ*, 500, 525
Scott, P. F., et al. 2003, *MNRAS*, 341, 1076
Taylor, A. C., et al. 2003, *MNRAS*, 341, 1066
Toffolatti, L., et al. 1998, *MNRAS*, 297, 117
Watson, R. A., et al. 2003, *MNRAS*, 341, 1057